Fourteenth International Conference on Domain Decomposition Methods
Editors: Ismael Herrera , David E. Keyes, Olof B. Widlund, Robert Yates

39. Interface Preconditioners for Splitting Interface Conditions in Air Gaps of Electrical Machine Models

H. De Gersem[1,2], S. Vandewalle[3], M. Clemens[1], T. Weiland[1]

1. Introduction. Electrical machine design is typically based on finite element (FE) simulations of steady-state working conditions. Motional eddy current effects are commonly resolved by transient simulation, which may be too expensive if only steady-state behaviour has to be simulated. This paper offers a time-harmonic FE approach for machines operating at steady-state, incorporating motional eddy current effects. The formulation incorporates interface conditions connecting the boundary of one stator model to the boundaries of several rotor models based on Fast Fourier Transforms and restriction operations. The matrix-free discretisation of the interface conditions excludes the use of algebraic iterative solution techniques. Instead, techniques related to iterative substructuring are proposed to solve the model.

2. Finite element machine models. Two common approaches for simulating electrical machines are the transient approach and the time-harmonic approach. The transient approach accounts for motional eddy currents by the Lagrange technique: between two successive time steps, the previous solution is azimuthally moved together with the rotor part. Accordingly, the interface conditions between stator and rotor are updated. The relative motion of both motor parts can be modelled by a moving band technique [5], a hybrid FE, boundary-element approach [8], discontinuous finite elements [1] or a sliding surface technique, possibly resolved by mortar finite elements [2]. Transient methods are however too expensive when only stationary operations have to be simulated.

For electrical machines excited by alternating current sources and rotating at constant velocities, formulations in frequency domain are preferred. The simplest case is when only one frequency f is present in the excitating voltages. Then, one can adopt the time-harmonic formulation

$$\nabla \times (\nu \nabla \times \underline{\mathbf{A}}) + \mathrm{j}\omega\sigma\underline{\mathbf{A}} = -\sigma\nabla\underline{V} \tag{2.1}$$

with the phasor $\underline{\mathbf{A}}$ related to the magnetic vector potential $\mathbf{A}$ by

$$\mathbf{A}(x,y,z,t) = \mathrm{Re}\left\{\underline{\mathbf{A}}(x,y,z)e^{\mathrm{j}\omega t}\right\} , \tag{2.2}$$

ν the reluctivity, σ the conductivity, $\underline{V}$ the phasor of the voltage and $\omega = 2\pi f$ the pulsation. Time-harmonic simulations are remarkably accurate and extremely efficient for the steady-state simulation of devices supplied with alternating currents. Unfortunately, accounting for motional effects in such simulations is not straightforward.

For many machines, a 2D FE model of the cross-section of the machine, extended with an equivalent circuit modelling the electric connections at the front and rear machine ends, achieves a sufficient accuracy [12]. Then, the vectorial PDE (2.1) simplifies to a scalar PDE in terms of the z-component $\underline{A}_z$ of $\underline{\mathbf{A}}$:

$$-\frac{\partial}{\partial x}\left(\nu\frac{\partial \underline{A}_z}{\partial x}\right) - \frac{\partial}{\partial y}\left(\nu\frac{\partial \underline{A}_z}{\partial y}\right) + \mathrm{j}\omega\sigma\underline{A}_z = \frac{\sigma}{\ell_z}\Delta\underline{V} \tag{2.3}$$

[1]Technische Universität Darmstadt, Computation Electromagnetics Laboratory, degersem/clemens/weiland@temf.tu-darmstadt.de
[2]H. De Gersem is working in the cooperation project "DA-WE1 (TEMF/GSI)" with the "Gesellschaft für Schwerionenforschung (GSI)", Darmstadt
[3]Katholieke Universiteit Leuven, Dep. Computer Science, stefan.vandewalle@cs.kuleuven.ac.be

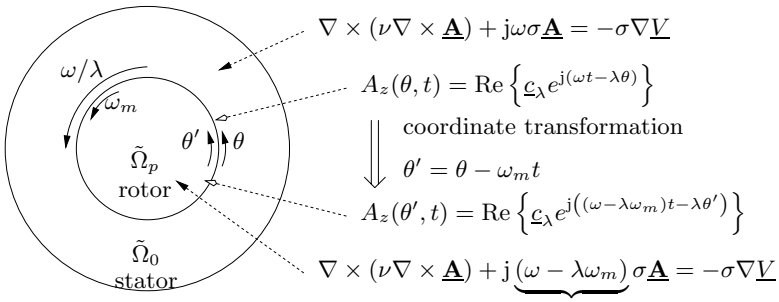

Figure 3.1: Slip transformation technique, illustrated for a simplified machine model.

with ℓ_z the device length and $\Delta\underline{V}$ the voltage drop between the machine's front and back side. The discretisation of (2.3) by linear triangular FE shape functions $N_i(x,y)$ yields the system of equations

$$K\underline{u} + \underline{g} = \underline{f} \tag{2.4}$$

with $\underline{u}$ containing the degrees of freedom for $\underline{A}_z$,

$$K_{ij} = \int_\Omega \left(\nu\frac{\partial N_i}{\partial x}\frac{\partial N_j}{\partial x} + \nu\frac{\partial N_i}{\partial y}\frac{\partial N_j}{\partial y} + \mathrm{j}\omega\sigma N_i N_j\right)\mathrm{d}\Omega\,, \tag{2.5}$$

$$\underline{f}_i = \int_\Omega \frac{\sigma}{\ell_z}\Delta\underline{V}\,N_i\,\mathrm{d}\Omega\,, \tag{2.6}$$

$$\underline{g}_i = -\int_{\partial\Omega} \nu\frac{\partial\underline{A}_z}{\partial n}\,N_i\,\mathrm{d}\Gamma \tag{2.7}$$

and $\partial/\partial n$ the normal derivative outward to Ω.

3. Slip transformation. Only in a very particular case, i.e., if the air gap field is a rotating wave, it is possible to account for motional eddy currents while keeping the classical time-harmonic formulation (2.3). Consider the simplified machine model of Fig. 3.1. Suppose the field at a circular interface between stator and rotor equals the rotating wave

$$A_z(\theta,t) = \mathrm{Re}\left\{\underline{c}_\lambda e^{\mathrm{j}(\omega t-\lambda\theta)}\right\} \tag{3.1}$$

with the phasor $\underline{c}_\lambda$, the pole pair number λ and the azimuthal coordinate θ along the interface. An observer attached to the stator experiences the wave as a cosine rotating at the velocity ω/λ along the interface. Consider a second observer attached to the rotor and hence inheriting its rotation at a constant mechanical velocity ω_m. The corresponding azimuthal coordinate θ' along the interface is related to θ by

$$\theta' = \theta - \omega_m t\,. \tag{3.2}$$

The rotating observer experiences the field at the interface as

$$A_z(\theta',t) = \mathrm{Re}\left\{\underline{c}_\lambda e^{\mathrm{j}((\omega-\lambda\omega_m)t-\lambda\theta')}\right\} \tag{3.3}$$

which is also a rotating wave with the same phasor and pole pair number, but with a different pulsation $\omega_{s,\lambda} = \omega - \lambda\omega_m$, called the *slip pulsation*. Hence, phenomena at the stator side induce phenomena at the rotor side at slip pulsation. Motional eddy currents are easily incorporated in (2.3) by replacing the pulsation ω by the slip pulsation $\omega_{s,\lambda}$ for the rotating

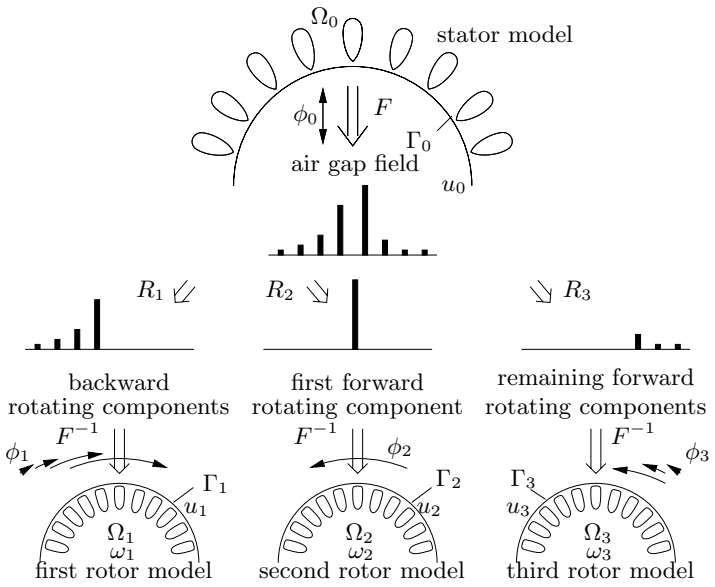

Figure 4.1: Scheme of the air gap flux decomposition approach illustrating the splitting of the total stator flux ϕ_0 into three parts ϕ_1, ϕ_2 and ϕ_3.

model parts. This procedure is called *slip transformation*. The assumption of a rotating wave form as field distribution in the air gap is approximately true for three-phase induction machines. Then, time-harmonic steady-state simulation with slip transformation commonly gives reliable results [4]. Other alternating current machines, e.g. single-phase induction machines, do not feature this property. Hence, time-harmonic simulation is at first glance not applicable.

4. Decomposition of the air gap field. The slip transformation technique is extendable to cases with more general air gap field distributions. The key point is to decompose the arbitrary air gap field into rotating field components and distribute these components towards distinct rotor models such that slip transformations can be defined for each rotating component independently [3]. Consider a model consisting of one stator model Ω_0 and n rotor domains Ω_p, $p = 1, \ldots, n$ (see Fig. 4.1 for an example with $n = 3$). The stator and rotor models share a circular interface Γ_b in the middle of the air gap. For each rotor domain, the slip pulsation $\omega_p = \omega - \lambda_p \omega_m$ is selected according to one of the field component present at Ω_p, i.e., the component with pole pair number λ_p. Because the stator windings do not experience eddy currents, ω_0 is set to zero. For each submodel independently, a FE subsystem is set up:

$$\begin{bmatrix} K_{p,aa} & K_{p,ab} \\ K_{p,ba} & K_{p,bb} \end{bmatrix} \begin{bmatrix} \underline{u}_{p,a} \\ \underline{u}_{p,b} \end{bmatrix} + \begin{bmatrix} 0 \\ \underline{g}_{p,b} \end{bmatrix} = \begin{bmatrix} \underline{f}_{p,a} \\ \underline{f}_{p,b} \end{bmatrix}, \quad p = 0, \ldots, n \tag{4.1}$$

where the subscripts a and b distinguish between degrees of freedom associated with inner nodes and degrees of freedom associated with nodes at Γ_b. Since in general $\omega_{p_1} \neq \omega_{p_2}$, the FE stiffness matrices for the rotor domains are different although they feature the same FE mesh and reluctivities. The subsystems are collected in the block diagonal matrices K_{aa}, K_{ab}, K_{ba} and K_{bb}, the vectors of unknowns $\underline{u}_a$ and $\underline{u}_b$, the boundary terms $\underline{g}_b$ and the load

vectors $\underline{f}_a$ and $\underline{f}_b$. For convenience, assume all submodels have equidistant and matching grids at Γ_b. An appropriate selection of rotating field components is performed by interface conditions applied at Γ_b:

$$F\underline{u}_{p,b} - R_p F \underline{u}_{0,b} = 0, \quad p = 1, \ldots, n \tag{4.2}$$

with F denoting the discrete Fourier transform and R_p a set of restriction operators such that $\sum_{p=1}^{n} R_p = I$. The interface conditions (4.2) take the distribution of $\underline{A}_z$ at the stator side of Γ_b ($\underline{u}_{0,b}$), transform this into harmonic components ($F\underline{u}_{0,b}$), next restrict these to a particular subset ($R_p F \underline{u}_{0,b}$) and finally equal this subset of harmonics to the harmonic components of the distribution of $\underline{A}_z$ at one of the rotor sides of Γ_b ($F\underline{u}_{p,b}$). The choices of the sets $\{R_p\}$ and $\{\omega_p\}$ are motivated by technical considerations [3]. For many electrical machines, only a few harmonics are responsible for the major machine behaviour whereas the remaining harmonics only have a marginal influence. Therefore, an important rotating field component λ_p is assigned to an individual rotor model Ω_p equipped with the corresponding slip pulsation $\omega_p = \omega - \lambda_p \omega_m$. The remaining harmonics are arbitrarily propagated to one of the already existing rotor models. Eddy current phenomena due to these harmonics are only approximately taken into account. The constraints (4.2) are added to the FE system (4.1). The boundary integral terms $\underline{g}_{p,b}$ are resolved in terms of a set of Lagrange multipliers $\underline{\xi}$, i.e., $\underline{g}_b = B^H \underline{\xi}$. The FE model including air gap flux decomposition corresponds to the saddle-point problem

$$\begin{bmatrix} K_{aa} & K_{ab} & 0 \\ K_{ba} & K_{bb} & B^H \\ 0 & B & 0 \end{bmatrix} \begin{bmatrix} \underline{u}_a \\ \underline{u}_b \\ \underline{\xi} \end{bmatrix} = \begin{bmatrix} \underline{f}_a \\ \underline{f}_b \\ 0 \end{bmatrix} \tag{4.3}$$

with

$$B = \begin{bmatrix} -R_1 F & F & & \\ \vdots & & \ddots & \\ -R_n F & & & F \end{bmatrix}. \tag{4.4}$$

Although the FE system part is complex symmetry, this property is not maintained in the system (4.3).

It is possible to eliminate the inner degrees of freedom $\underline{u}_{p,a}$ with respect to the degrees of freedom $\underline{u}_{p,b}$ at Γ_b for each submodel independently. The Schur complement subsystems $D_p \underline{u}_{p,b} = \underline{q}_p$ with stiffness matrices $D_p = K_{p,bb} - K_{p,ba} K_{p,aa}^{-1} K_{p,ab}$ and load vectors $\underline{q}_p = \underline{f}_{p,b} - K_{p,ba} K_{p,aa}^{-1} \underline{f}_{p,a}$, are collected in $D\underline{u}_b = \underline{q}$. The system with interface conditions reads

$$\begin{bmatrix} D & B^H \\ B & 0 \end{bmatrix} \begin{bmatrix} \underline{u}_b \\ \underline{\xi} \end{bmatrix} = \begin{bmatrix} \underline{q} \\ 0 \end{bmatrix}. \tag{4.5}$$

Two other reductions can be considered: one eliminating all $\underline{u}$ and hence left with the Lagrange multipliers only:

$$S\underline{\xi} = BD^{-1}\underline{q} \tag{4.6}$$

with $S = BD^{-1}B^H$ and one eliminating all $\underline{\xi}$ and $\underline{u}_{p,b}$, $p = 1, \ldots, n$ and hence left with an independent set of degrees of freedom for the magnetic vector potential:

$$\begin{bmatrix} I & \\ & Q^H \end{bmatrix} \begin{bmatrix} K_{aa} & K_{ab} \\ K_{ba} & K_{bb} \end{bmatrix} \begin{bmatrix} I & \\ & Q \end{bmatrix} \begin{bmatrix} \underline{u}_a \\ \underline{u}_{0,b} \end{bmatrix} = \begin{bmatrix} I & \\ & Q^H \end{bmatrix} \begin{bmatrix} \underline{f}_a \\ \underline{f}_b \end{bmatrix}; \tag{4.7}$$

$$Q^H = \begin{bmatrix} I & F^H R_1 F & \cdots & F^H R_n F \end{bmatrix} \tag{4.8}$$

with $F^H = F^{-1}$ the inverse discrete Fourier transform. The operator Q assigns a particular set of rotating field components generated by the stator winding at Γ_b to each of the rotor sides of Γ_b.

5. Solution of the coupled system. For computational efficiency, the operators F, F^H, R_p and B are not constructed as matrices. Instead, we apply Fast Fourier Transforms (FFTs) for F and F^H and explicit restrictions for R_p. This excludes the usage of direct solution and algebraic preconditioning techniques. The coupled systems (4.3), (4.5), (4.6) and (4.7) are neither Hermitian nor complex symmetric and are solved by a preconditioned Bi-Conjugate Gradient Stabilised (BiCGStab) method [10]. An appropriate algebraic multigrid preconditioner $\tilde{K}_{\mathrm{AMG}}$ is available for the FE matrix part with circuit equations [9]. The block corresponding to the Lagrange multipliers has to be preconditioned by an approximation to system S [11, 13].

The constraint equation $B\underline{u}_b = 0$ enforces flux continuity whereas the relation $\underline{g}_b = B^H\underline{\xi}$ ensures the correct distribution of the magnetic field strength. The Lagrange multipliers represent the Fourier coefficients of the boundary integral terms $\underline{g}_{p,b}$ of the individual rotor domains. This physical interpretation indicates a possible problem-based preconditioning technique. A preconditioner is constructed based on a classical analytical model for cylindrical induction machines which neglects the stator and rotor slotting and the saturation of the ferromagnetic materials. The approximate model consists of a set of concentric rings, each with equivalent homogeneous material properties [7]. Here, the stator and the rotor are represented by a single homogeneous domain: the stator domain $\tilde{\Omega}_0$ with equivalent reluctivity $\tilde{\nu}_{\mathrm{st}}$ and the rotor domains $\tilde{\Omega}_p$ with equivalent reluctivities $\tilde{\nu}_{\mathrm{rt}}$, equivalent conductivities $\tilde{\sigma}_{\mathrm{rt}}$ and the slip pulsations ω_p (Fig. 3.1). The analytical relations for the Fourier coefficients $\underline{\tilde{h}}_{p,b,\lambda}$ of the magnetic field strength at the stator and rotor sides of Γ_b with respect to the Fourier coefficients $\underline{\tilde{a}}_{p,b,\lambda}$ of $\underline{A}_z$ at Γ_b are

$$\underline{\tilde{h}}_{0,b,\lambda} = \underline{\tilde{\nu}}_{\mathrm{st}} \frac{\lambda}{r_b} \frac{\gamma^\lambda + \gamma^{-\lambda}}{\gamma^\lambda - \gamma^{-\lambda}} \underline{\tilde{a}}_{0,b,\lambda} \tag{5.1}$$

$$\underline{\tilde{h}}_{p,b,\lambda} = -\underline{\tilde{\nu}}_{\mathrm{rt}} \frac{\beta_p I'_\lambda(\beta_p r_b)}{I_\lambda(\beta_p r_b)} \underline{\tilde{a}}_{p,b,\lambda} \tag{5.2}$$

with the factor $\beta_p = \sqrt{\mathrm{j}\omega_p \sigma_{\mathrm{rt}}/\nu_{\mathrm{rt}}}$, I_λ the modified Bessel function of order λ, $\gamma = r_b/r_s$ the stator form factor, r_b the radius of Γ_b and r_s the outer radius of the stator. Weighting (5.1) and (5.2) by the FE shape functions and integration along Γ_b yields an approximate relation between $\underline{\tilde{a}}_{p,b,\lambda}$ and the weighted magnetic field strengths $\underline{\tilde{g}}_{p,b,\lambda}$ they exert at the stator and rotor sides of Γ_b:

$$\underline{\tilde{g}}_{0,b,\lambda} = \underline{\tilde{\nu}}_{\mathrm{st}} \Delta\theta \kappa_\lambda \lambda \frac{\gamma^\lambda + \gamma^{-\lambda}}{\gamma^\lambda - \gamma^{-\lambda}} \underline{\tilde{a}}_{0,b,\lambda} \tag{5.3}$$

$$\underline{\tilde{g}}_{p,b,\lambda} = \underline{\tilde{\nu}}_{\mathrm{rt}} \Delta\theta \kappa_\lambda \frac{\beta_p r_b I'_\lambda(\beta_p r_b)}{I_\lambda(\beta_p r_b)} \underline{\tilde{a}}_{p,b,\lambda} \tag{5.4}$$

with $\kappa_\lambda = \frac{\sin(\lambda\Delta\theta/2)}{\lambda\Delta\theta/2}$ and $\Delta\theta$ the angle between two successive FE nodes at Γ_b. Expressions (5.3) and (5.4) are gathered in the matrix systems $\underline{\tilde{g}}_{p,b} = \tilde{H}_p \underline{\tilde{a}}_{p,b}$, further collected in $\underline{\tilde{g}}_b = \tilde{H}\underline{\tilde{a}}_b$, combined into a preconditioner for D and inserted in an approximation to S:

$$\tilde{D} = \mathrm{diag}\left(F^H\tilde{H}_0F, F^H\tilde{H}_1F, \ldots, F^H\tilde{H}_pF\right), \tag{5.5}$$

$$\tilde{S}_{\mathrm{dyn}} = B\tilde{D}^{-1}B^H = \mathrm{diag}\left(\tilde{H}_1^{-1} + R_1\tilde{H}_0^{-1}, \ldots, \tilde{H}_n^{-1} + R_n\tilde{H}_0^{-1}\right) \tag{5.6}$$

where the factors R_p introduce appropriate weights in order to account for the flux splitting at Γ_b. A similar approximation $\tilde{S}_{\mathrm{stat}}$ is built based on a static analytical model with $\omega_p = 0$ for all rotor models. Since all matrices in (5.6) are diagonal, the cost of applying $\tilde{S}_{\mathrm{dyn}}^{-1}$ or $\tilde{S}_{\mathrm{stat}}^{-1}$ to a vector is negligible. The systems (4.3), (4.5) and (4.6) can be solved by BiCGStab

Table 6.1: Number of iteration of BiCGStab with a block Jacobi preconditioner applied to a small motor model.

		1 rotor domain			6 rotor domains			12 rotor domains		
conductivity σ in S/m		50	500	5000	50	500	5000	50	500	5000
K	S	3	3	3	3	3	3	3	3	3
$\tilde{K}_{\mathrm{AMG}}$	S	6	6	6	7	6	6	7	6	6
$\tilde{K}_{\mathrm{ILU(0)}}$	S	51	46	24	125	109	57	173	145	57
K	$\tilde{S}_{\mathrm{ILU(0)}}$	21	19	13	200	184	98	198	195	100
$\tilde{K}_{\mathrm{ILU(0)}}$	$\tilde{S}_{\mathrm{ILU(0)}}$	43	43	24	59	71	50	61	101	50
K	$\tilde{S}_{\mathrm{stat}}$	5	5	7	5	5	7	5	5	5
$\tilde{K}_{\mathrm{AMG}}$	$\tilde{S}_{\mathrm{stat}}$	6	14	20	12	24	53	12	24	55
$\tilde{K}_{\mathrm{ILU(0)}}$	$\tilde{S}_{\mathrm{stat}}$	51	52	44	110	167	200	150	192	198
K	$\tilde{S}_{\mathrm{dyn}}$	3	3	3	3	3	3	3	3	3
$\tilde{K}_{\mathrm{AMG}}$	$\tilde{S}_{\mathrm{dyn}}$	7	6	6	7	6	6	7	6	6
$\tilde{K}_{\mathrm{ILU(0)}}$	$\tilde{S}_{\mathrm{dyn}}$	78	49	34	125	109	57	173	145	57

using as a preconditioner $\mathrm{diag}(\tilde{K}, \tilde{S})$, $\mathrm{diag}(\tilde{D}, \tilde{S})$ and $\tilde{S}$ respectively. We prefer to solve (4.3), preconditioned by $\mathrm{diag}(\tilde{K}, \tilde{S})$.

6. Numerical experiments. The performance of the preconditioner is tested for a small technical induction machine model (Table 6.1). The system (4.3) is solved by BiCGStab and preconditioned by a block Jacobi preconditioner of which the diagonal blocks are indicated in the table. The dependence of the number of iterations is checked with respect to the number of rotor domains and the importance of the eddy current effects, characterised by the conductivity. The system (4.3) preconditioned by $\mathrm{diag}(K, S)$ has three eigenvalues and, hence, converges in 3 steps [6]. Replacing the exact solution of the FE system part by the AMG preconditioner $\tilde{K}_{\mathrm{AMG}}$ causes only a small increase of the number of iterations. The next numerical test with the Incomplete LU-preconditioner without fill-in (ILU(0)) $\tilde{K}_{\mathrm{ILU(0)}}$ indicates that, for this problem, the choice of a good preconditioner for the FE part is more critical than the choice of the preconditioner for the Lagrange multiplier space. Notice that the construction of a Schur complement preconditioner using the preconditioner for the FE part, e.g. $\tilde{S}_{\mathrm{ILU(0)}} = B\tilde{K}^{-1}_{\mathrm{ILU(0)}}B^H$, is in practice too expensive. The number of iterations with the ILU(0) preconditioner may decrease with respect to increasing conductivity since then, the FE system becomes more diagonally dominant which explains the better performance of ILU(0). The last two numerical experiments demonstrate the performance of the preconditioners $\tilde{S}_{\mathrm{stat}}$ and $\tilde{S}_{\mathrm{dyn}}$ based on a static and dynamic analytical model respectively. For the static Schur complement preconditioner $\tilde{S}_{\mathrm{stat}}$, the number of iterations increases significantly with the conductivity due to the fact that eddy current effects are neglected in the Schur complement preconditioner. The more sophisticated analytical model from which $\tilde{S}_{\mathrm{dyn}}$ is constructed, leads to an iteration number independent from the conductivity. Because of the factors R_p in the Schur complement preconditioners, the number of iterations is not affected by the number of rotor domains.

7. Capacitor motor. The air gap flux decomposition technique is applied to a capacitor motor (Fig. 7.1). The fundamental forward and backward rotating air gap flux components, i.e., those with pole pair numbers 1 and -1, produce the most important torque components. Two rotor models are considered: Ω_1 for all components with positive pole pair numbers and Ω_2 for all components with negative pole pair numbers (Fig. 7.2). At Ω_1, the slip pulsation $\omega_1 = \omega - \omega_m$ is applied whereas at Ω_2, the slip pulsation $\omega_2 = \omega + \omega_m$, is used. Hence, only motional eddy current effects with respect to the fundamental rotating air gap

(a)

(b)

Figure 7.1: (a) Stator and (b) rotor of the capacitor motor.

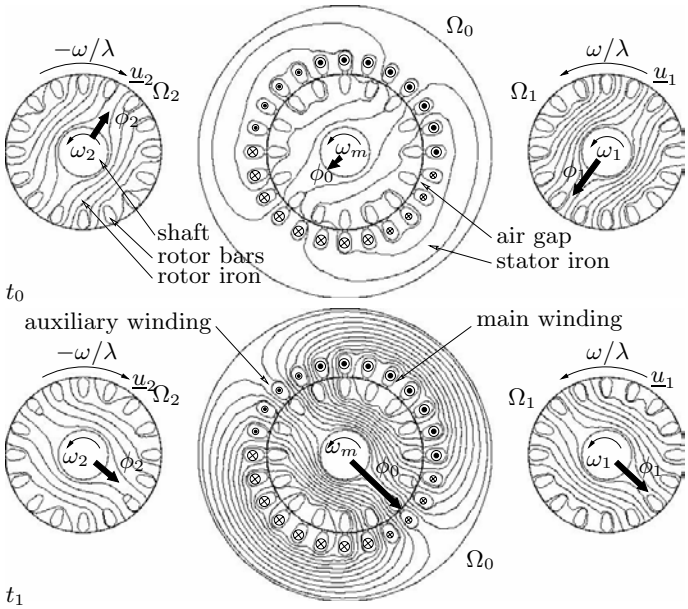

Figure 7.2: Plot of the magnetic flux lines at t_0 and t_1 of a capacitor motor operating at 1500 rotations per minute.

field components are correctly taken into account. The flux patterns plotted at two instants of time shifted over a quarter of a period, show the true alternating true rotor field ϕ_0 and the rotating forward and backward field components ϕ_1 and ϕ_2.

8. Conclusions. Motional eddy currents are considered within time-harmonic FE machine models by decomposing the air gap flux into rotating components and distributing these to independent rotor models. An appropriate solution scheme for the FE system incorporating interface conditions based on FFTs, consists of the BiCGStab algorithm and block preconditioning based on AMG for the FE part and an approximation for the interface Schur complement matrix based on approximate analytical machine models.

REFERENCES

[1] P. Alotto, A. Bertoni, I. Perugia, and D. Schötzau. Discontinuous finite element methods for the simulation of rotating electrical machines. *COMPEL*, 20(2):448–462, 2001.

[2] A. Buffa, Y. Maday, and F. Rapetti. A sliding mesh-mortar method for a two dimensional eddy-currents model of electric engines. Math. Meth. Anal. Num. (submitted), 1999.

[3] H. De Gersem and K. Hameyer. Air-gap flux splitting for the time-harmonic finite element simulation of single-phase induction machines. IEEE Trans. Magn., in print, mar 2002.

[4] R. De Weerdt, E. Tuinman, K. Hameyer, and R. Belmans. Finite element analysis of steady state behavior of squirrel cage induction motors compared with measurements. *IEEE Trans. Magn.*, 33(2):2093–2096, March 1997.

[5] A. Demenko. Movement simulation in finite element analysis of electric machine dynamics. *IEEE Trans. Magn.*, 32(3):1553–1556, May 1996.

[6] B. Fischer, A. Ramage, D. J. Silvester, and A. J. Wathen. Minimum residual methods for augmented systems. *BIT*, 38(3):527–543, 1998.

[7] E. M. Freeman. Equivalent circuits from electromagnetic theory: low-frequency induction devices. *IEE Proc.*, 121(10):1117–1121, October 1974.

[8] S. Kurz, J. Fetzer, G. Lehner, and W. M. Rucker. A novel formulation for 3D eddy current problems with moving bodies using a Lagragian description and FEM-BEM coupling. *IEEE Trans. Magn.*, 34(5):3068–3073, September 1998.

[9] D. Lahaye, K. Hameyer, and S. Vandewalle. An algebraic multilevel preconditioner for field-circuit coupled problems. *IEEE Trans. Magn.*, March 2002. in print.

[10] G. L. Sleijpen, H. A. Van der Vorst, and D. R. Fokkema. BICGSTAB(l) and other hybrid Bi-CG methods. *Num. Alg.*, 7:75–109, 1994.

[11] B. F. Smith, P. E. Bjørstad, and W. Gropp. *Domain Decomposition: Parallel Multilevel Methods for Elliptic Partial Differential Equations*. Cambridge University Press, 1996.

[12] I. A. Tsukerman, A. Konrad, G. Meunier, and J.-C. Sabonnadière. Coupled field-circuit problems: trends and accomplishments. *IEEE Trans. Magn.*, 29(2):1701–1704, March 1993.

[13] J. Xu and J. Zou. Some nonoverlapping domain decomposition methods. *SIAM Review*, 40:857–914, 1998.